

Enhancement of top production in $e^+e^- \rightarrow t\bar{t}$

Lali Chatterjee^{1,2} and Cheuk-Yin Wong¹

¹*Oak Ridge National Laboratory, Oak Ridge, TN 37831*

and

²*Jadavpur University, Calcutta 700032, India.*

Abstract

We investigate $e^+e^- \rightarrow t\bar{t}$ by taking into account wave function distortion effects in the near-threshold region and interpolating the correction factor to the high-energy perturbative QCD region. The strong color attraction between the color singlet t and \bar{t} enhances the cross section over the tree level results near threshold. The rise of the cross section near the threshold is smoothed by the effects of the large top width and below-threshold resonances. The reliability of the prediction is well assessed by comparing with experimental R ratios for lighter quark production at lower energies. The cross sections obtained here using the reported values of the top mass, can be used directly for New Linear Collider (NLC) projections.

Typeset using REVTeX

I. INTRODUCTION

Recent reports of the observation of the top quark, with a mass of 174 GeV [1], provoke improved theoretical studies of the top flavor. The planned and proposed experimental focus for the next decade to develop and understand top physics and top characteristics add impetus to theoretical investigations [2–7]. The super-heavy value of the top mass also opens up new vistas of electroweak physics and possibilities for probing for effects beyond the Standard Model. Many special features of the top have been studied recently [8–12]. Being heavier than the W , the top is extremely susceptible to weak decay by the $t \rightarrow W^+b$ channel. This large width distinguishes it from its doublet partner b , as well as the lower generation quarks and will lead to the disappearance of the sharp resonance structure corresponding to below-threshold resonances, as one transits from the c and b to the t flavor. Yet another feature, special to the top sector is the reliability of perturbative QCD to probe its bound and continuum states as the non-perturbative regime does not contribute effectively at the very short distances characterized by $1/m_t$ for top flavor production.

Careful analyses of higher-order QCD corrections for production of heavy quarks with a finite mass have been carried out [13–15] which indicate that the next-to-leading order corrections are very large when the relative velocity between the top quark and the top antiquark is small. For such massive fermions near the threshold, the distortion of the outgoing relative wavefunctions between the top quark and the top antiquark, due to the strong color field connecting them, would be a dominant correction to the $t\bar{t}$ production processes. This can be understood in terms of ‘Coulomb gluons’ analogous to those acting between c and \bar{c} in the J/ψ systems and between b and \bar{b} in Υ . The importance of such Coulomb effects for heavy quark production processes has been recognized earlier in the study of heavy quark productions in bound and continuum states [16–19,8].

In the present work we expand on these aspects and predict the rates for $t\bar{t}$ production by virtual γ and Z exchange in e^+e^- collider experiments, according to $e^+e^- \rightarrow \gamma^*(Z^*) \rightarrow Q\bar{Q}$, including the important near-threshold region. The two loop modified running coupling

constant $\alpha_s(q^2)$ in the five flavor theory is used and the threshold QCD corrections are folded into the high energy results by an interpolation formula. Effects of top width and below-threshold resonances are included. Corrections for running of the QED coupling have been incorporated. The cross section obtained here using the latest top mass, can be used for future e^+e^- collider projections. Results are extended to the charm and beauty flavors and applied to the familiar R parameter for comparison with experiment.

II. TREE LEVEL CROSS SECTION

The differential cross section for $e^+e^- \rightarrow Q\bar{Q}$ above threshold at a center-of-mass energy \sqrt{s} is given at the tree level by Eqs. (24.11)-(24.19) of Ref. [20],

$$\frac{d\sigma(s)}{dz} = \frac{3\pi\alpha^2}{4s} \left(\frac{e_Q}{e}\right)^2 \beta D, \quad (1)$$

where $z = \cos\theta$, and m_Q and e_Q are the quark mass and charge, and we have included the three different colors of the quark-antiquark pair. In Eq. (1), the quantity β is

$$\beta = \sqrt{1 - \frac{4m_Q^2}{s}},$$

the quantity D is

$$D = e_Q^2 A - 2e_Q \chi_1 [VV_f A - 2a_f \beta z] + \chi_1^2 B, \quad (2)$$

where

$$A = 1 + z^2 + (1 - \beta^2)(1 - z^2),$$

$$B = V_f^2(1 + V^2)A + \beta^2 a_f^2(1 + V^2)[1 + z^2] - 8\beta V V_f a_f z,$$

$$\chi_1 = \frac{x}{16 \sin^2 \theta_w \cos^2 \theta_w},$$

$$V = -1 + 4 \sin^2 \theta_w,$$

$$V_f = 2T_{3f} - 4e_Q \sin^2 \theta_w,$$

$a_f = 2T_{3f} = 1$ for the top, and θ_w is the Weinberg angle. The quantity x contains the Z mass m_Z as

$$x = \frac{s}{s - m_Z^2}.$$

Integrating over the angle, as we are not probing the asymmetry but the top production, we obtain

$$\sigma(s) = \frac{4\pi\alpha^2}{s} \left(\frac{e_Q}{e}\right)^2 H\beta \quad (3)$$

where

$$H = \left(1 + \frac{1 - \beta^2}{2}\right) \left\{ e_Q^2 - 2e_Q\chi_1 VV_f + \chi_1^2 V_f^2 (1 + V^2) \right\} + \beta^2 a_f^2 (1 + V^2). \quad (4)$$

The above expressions are obtained using plane waves for all the fermions. It is however well recognized that the lowest order diagrams are inadequate to describe the quark sector, because of the large value of the QCD coupling constant α_s . Even for light quarks, the next-to-leading order radiative corrections for such production vertices predict an increase in the lowest order values, according to the correction factor $(1 + \alpha_s/\pi)$, where α_s is the strong coupling constant [21]. These corrections, obtained painstakingly as the residual quantities after cancellation of singularities, unfortunately require the massless or chiral limit for their applicability. It is easy to see that the massless limit is not a desirable *modus operandi* when dealing the top flavor near the threshold, with its mass of 174 GeV.

The large mass of the top quark assures the importance of the part of the vertex correction due to the exchange of longitudinal gluons between the top quark and the top antiquark at the $\gamma^* t\bar{t}$, or $Z^* t\bar{t}$ vertex, near the $t\bar{t}$ threshold at around 350 GeV. This exchange can be represented by a potential that acts between the t and \bar{t} .

III. VERTEX CORRECTION FACTOR

If we consider direct materialization of a quark-antiquark pair by decay of an intermediate virtual photon for instance, the process is characterized by a region of very small relative

$Q\bar{Q}$ separations, at a $Q\bar{Q}$ distance of $\sim \alpha/\sqrt{s}$. The effective part of the $Q\bar{Q}$ interaction in this region of small relative separation associated with the production process is the inverse- r , Coulomb-like term. The linear part of the potential, that serves to effect the binding and impose confinement, controls the large r behavior [22,23] and needs not be considered in the collapsed spatial zone comprising the annihilation or production vertex. This is further augmented by the short lifetime of the t and \bar{t} that prohibits their moving away beyond the perturbative range.

Upon expressing the one-gluon exchange potential between the quark and the antiquark in the $1/r$ Coulomb-like form, one can obtain exact solution for the wavefunction [24] and extract the $r = 0$ part to correct the plane waves used in the Born diagram for their distortion in the color field. This procedure corrects for the distortion effect to all orders, and the resulting corrections can extend the applicability of PQCD for this process to the near-threshold region. We have discussed these correction factors for the lighter quark annihilation and production in a separate work [25]. Though we restrict the main analysis to top flavor, the results can be easily extended to lighter flavors, and are seen below to be compatible with charm and beauty production near their relevant thresholds.

We use a suitable short distance color potential of the Coulomb type,

$$V(r) = \frac{-\alpha_{\text{eff}}}{r},$$

where

$$\alpha_{\text{eff}} = C_f \alpha_s(q^2),$$

C_f is the appropriate color factor, and α_s is the two-loop modified running QCD coupling constant and can be calculated from [26]

$$\alpha_s(q^2) = \frac{4\pi}{(11 - 2n_f/3) \ln(q^2/\Lambda^2)} \left(1 - \frac{2(51 - 19n_f/3) \ln[\ln(q^2/\Lambda^2)]}{(11 - 2n_f/3)^2 \ln(q^2/\Lambda^2)} \right), \quad (5)$$

where q^2 is identified as s and Λ is taken to be $\Lambda^{(5)} = 195$ MeV for top production.

For outgoing final states relevant to a produced $Q\bar{Q}$ pair, the wave function of the quark Q in the field of the antiquark \bar{Q} is given by [24]

$$\psi = N e^{i\mathbf{p}\cdot\mathbf{r}} \left(1 - \frac{i}{2E} \boldsymbol{\alpha} \cdot \nabla\right) u F(-i\xi, 1, -i(pr + \mathbf{p} \cdot \mathbf{r})), \quad (6)$$

where u is the spinor for the free quark, F is the confluent hypergeometrical function and N is the normalization constant given by

$$|N|^2 = \frac{2\pi\xi}{1 - e^{-2\pi\xi}},$$

where

$$\xi = \alpha_{\text{eff}}/v,$$

and v is the relative velocity between the quark and the antiquark given by [25]

$$v = \frac{\sqrt{1 - 4m_Q^2/s}}{1 - 2m_Q^2/s}. \quad (7)$$

The square of the wavefunction taken at contact can be obtained as a generalization of the familiar ‘Gamow-Sommerfeld factor’ [27] as

$$K^{(f)} = |\psi(0)|^2 = \frac{2\pi\xi}{1 - e^{-2\pi\xi}} (1 + \alpha_{\text{eff}}^2), \quad (8)$$

where spins of both quarks have been averaged over and the superscript (f) is to indicate that this is the correction factor for quark-antiquark production in the final state [25].

In order to obtain a generalized correction factor, that is valid not only when Q and \bar{Q} have low relative velocities, but also have large relative velocities, we use the interpolation technique suggested by Schwinger [28]. In the massless quark limit, the next-to-leading order QCD corrections to production of $q\bar{q}$ at high energies is given by the correction factor $K^{(f)} = (1 + \alpha_s/\pi)$ [21]. The transition of the QCD corrections from the correction factor $K^{(f)}$ of Eq. (8) at low relative velocities, to the $(1 + \alpha_s/\pi)$ behavior at relativistic velocities can be accommodated with the introduction of an interpolative function $f^{(f)}(v)$, where

$$f^{(f)}(v) = \alpha_{\text{eff}} \left[\frac{1}{v} + v \left(-1 + \frac{3}{4\pi^2} \right) \right]. \quad (9)$$

The generalized QCD correction factor, applicable at all relative velocities can be written as

$$K^{(f)} = \frac{2\pi f^{(f)}(v)}{1 - \exp[-2\pi f^{(f)}(v)]} (1 + \alpha_{\text{eff}}^2). \quad (10)$$

Incorporating the distortion correction, equation (3) for $t\bar{t}$ formation by the electroweak channels becomes, at energies above $2m_Q$,

$$\sigma(s) = K^{(f)} \frac{4\pi\alpha^2}{s} \left(\frac{e_Q}{e}\right)^2 \sqrt{1 - \frac{4m_Q^2}{s}} H \quad (11)$$

For virtual photon or Z mediated processes, the quark-antiquark pair must be in color-singlet states. The color factor C_f has the value $4/3$ and the one-gluon exchange potential is attractive between the quark and antiquark. Due to this attractive nature of the color-singlet interaction, the correction factor (10) enhances top production over the tree level expectations. As in earlier analyses [8], [16]- [19], there is a large enhancement of top flavor production near threshold due to the wavefunction distortion by this attractive color field.

It may be noted that in the large ξ limit, the correction factor in Eq. (11) takes the form $\pi\xi = \pi C_f \alpha_s / v$. As $v \rightarrow 0$, corrected $\sigma(s)$ of Eq. (11) does not diverge to infinity, because the $\sqrt{1 - 4m_Q^2/s}$ term of (11) cancels with the corresponding term in the velocity in Eq. (7). This cancellation of the Coulomb singularity by the phase space factor has been discussed in the context of $Q\bar{Q}$ formation by $q\bar{q}$ annihilation in hadronic collisions [13]. In the absence of the vertex correction, the top production rate would plunge to zero at threshold, whereas with the correct inclusion of distortion effects, the cross section attains a relatively constant value. The introduction of the bound toponium states and the finite top width modifies this constancy as one approaches the threshold and softens considerably the cut-off at the threshold.

IV. INCLUSION OF THE TOP DECAY WIDTH AND BELOW-THRESHOLD BOUND STATES

The large weak decay rate of the top and the contribution of below-threshold bound states should be included for correct prediction of near-threshold top production. In the

Standard Model, the decay rate for the top by the dominant $t \rightarrow W^+b$ mode can be written as [29]

$$\Gamma_t = \frac{G_f m_t^3}{8\pi\sqrt{2}} |V(tb)|^2 \frac{2k}{m_t} L, \quad (12)$$

where

$$L = [1 - (m_b/m_t)^2]^2 + [1 + (m_b/m_t)^2][(m_w/m_t)^2] - 2(m_w/m_t)^4, \\ k = \frac{\left([m_t^2 - (m_w + m_b)^2]^{1/2}[m_t^2 - (m_w - m_b)^2]^{1/2}\right)}{2m_t},$$

and $V(tb)$ is the Standard Model mixing parameter which can be taken to be unity.

The effects of the top width can be introduced by including the contribution from all other energies to the cross section at the energy under consideration. The cross section at a given energy \sqrt{s} should then be written as

$$\sigma(s) = \sum_i \sigma_i(E_i) J_i(s, E_i), \quad (13)$$

where $\sigma_i(E_i)$ is the total cross section for state E_i and $J_i(s, E_i)$ is the normalized Breit-Wigner distribution

$$J_i(s, E_i) = \frac{1}{\pi} \frac{\Gamma/2}{[(\sqrt{s} - 2m_t - E_i)^2 + (\Gamma/2)^2]}.$$

The summation runs over all state energies E_i and the width Γ refers to the decay of the combined $t\bar{t}$ system and is given by $\Gamma = 2\Gamma_t$. The cross section can be devolved into a summation $\sigma_b(s)$ over all discrete bound states and an integration $\sigma_c(s)$ over all continuum states as

$$\sigma(s) = \sigma_b(s) + \sigma_c(s). \quad (14)$$

Integrating over the continuum, the open or continuum cross section, including the top width effects can be written as

$$\sigma_c(s) = K^{(f)} \frac{4\pi\alpha^2}{s} \left(\frac{e_Q}{e}\right)^2 \beta_H J_c(s), \quad (15)$$

where

$$J_c(s) = \frac{1}{\pi} \left\{ \frac{\pi}{2} + \tan^{-1} \left(\frac{\sqrt{s} - 2m_t}{\Gamma} \right) \right\}.$$

In this case the width softens the sharp step-function type onset of continuum production into a smooth leakage into the region below the threshold.

The case of the bound states requires the input of the bound state energies and wavefunctions. It is expected that the attractive color field between the produced $t\bar{t}$ will form bound toponium states like the charmonium and bottonium systems with similar spectroscopic properties. The $t\bar{t}$ system differs from the $c\bar{c}$ and $b\bar{b}$ in two important respects. Due to the large virtuality of the process for the pair with top flavor and the correspondingly large QCD scale, characterized by $1/m_t$, the QCD perturbative coupling is considerably smaller than that for the lighter $q\bar{q}$ pairs and PQCD is justified. Secondly, the large top mass and resulting large decay probability into the W and b is a characteristic not shared by the pairs with b or c flavor.

The large magnitude of the momentum transfer allows us to describe the lowlying toponium bound states as those in the attractive perturbative Coulomb-like inter-quark color field as nonperturbative effects are not manifested at the short distances applicable to $t\bar{t}$ materialization. The effects of the gluon condensate have been studied by [12,8] and shown to be small. The work in [12] further establishes the validity of the Coulomb color potential for the toponia states.

Bound states in the $t\bar{t}$ color field can be described simply by Coulomb-like wavefunctions and energy levels. Using the same perturbative Coulomb-like potential as for the continuum, we can write for the energy of the n th bound state

$$E_n = -\frac{\mu\alpha_{\text{eff}}^2}{2n^2},$$

where μ is the reduced mass of the quarks. The wavefunction at $t\bar{t}$ contact can be written as [10]

$$|\psi_n(0)|^2 = \frac{1}{\pi} \left(\frac{\mu\alpha_{\text{eff}}}{n} \right)^3.$$

The total cross section for below-threshold resonance toponium production can then be written as [10]

$$\sigma_n = \frac{4\pi\alpha^2}{s} \left(\frac{e_Q}{e} \right)^2 \frac{3\pi m_t \alpha_{\text{eff}}^3}{4n^3}.$$

Introducing the resonances and the finite width, the cross section for the n th bound state becomes $\sigma_n(E_n)J_n(s, E_n)$ and Γ continues to be twice the top weak decay width as branching ratios to any other channel is negligible. The effect of the large magnitude of the top width of 1.5 GeV, is to smear out the resonance structure of the bound states and yield a smooth contribution.

The total production cross section sums the contribution of bound and continuum states. The resulting continuum cross sections are enhanced over the tree level values, the effect being most pronounced just above threshold and tapering off at very high energies. This is demonstrated in Fig. 1, where the total cross section for $e^+e^- \rightarrow t\bar{t}$, calculated by including the width effects and the QCD correction factor $K^{(f)}$ for the continuum states, is shown as the solid curve and the tree-level cross section for the continuum states is shown as the dashed curve for comparison. The large enhancement at low relative $t\bar{t}$ velocities induced by the distortion corrections in this region is clearly visible. The cross sections remain enhanced over the lowest order results as the energy increases. At higher energies the cross sections fall with the usual inverse s behavior.

We also present in Fig. 2 the detailed threshold behavior, with the separate contributions from the bound and the continuum states. As remarked earlier, the large top width smears out the resonance structure into a smooth contribution. These results are in conformity to earlier investigations of the threshold region, that were spread over wide-ranging possible top mass values [8–11].

We have used the reported central value of 174 GeV for the top mass [1]. This value is in line with the earlier direct searches that set a lower limit $m_t > 131$ GeV/ c^2 [30] and with the global fits to precision electroweak fits that give a central value of $m_t = 177$ GeV/ c^2 [31]. The accepted value of 91.17 GeV [26] has been used for the Z mass and the weak mixing

angle has been taken as $\eta = 0.225$ [32,26].

The correction factor $K^{(f)}$ used here is similar to those used earlier [16–19,8,28], for lighter quarks, with small differences. We use relativistic kinematics to interpolate the correction factor to the high-energy region. Our results are in general agreement with the earlier works, but serve to quantify and extend them using the latest values of the electroweak parameters and top mass and are directly applicable over a wide range of energies.

V. LIGHTER HEAVY QUARKS

In order to demonstrate the reliability of our predictions for top quark production, it is necessary to show that the large enhancement of heavy quark production is consistent with experimental data. Therefore, we extend our analysis to cover the lower energy region spanned by experiments for heavy quark formation by e^+e^- annihilation.

The most appropriate quantity to use for meaningful comparison with experiment is the ratio of hadronic to leptonic (muonic) branching ratios, commonly designated as R ,

$$R = \frac{\sigma(e^+e^- \rightarrow \text{hadrons})}{\sigma(e^+e^- \rightarrow \mu^+\mu^-)}.$$

The numerator takes the form

$$\sigma(e^+e^- \rightarrow \text{hadrons}) = N_c \sum_f K^{(f)}(q_f) \sigma_f(s),$$

where for the continuum states

$$\sigma_f(s) = \left(\frac{e_f}{e}\right)^2 \frac{4\pi}{3s} \alpha^2 \sqrt{1 - \frac{4m_f^2}{s}} \left(1 + \frac{2m_f^2}{s}\right) \theta\left(1 - \frac{4m_f^2}{s}\right).$$

In this case the total widths being of MeV order have no perceptible influence on flavor production cross sections. Nor do they distort the resonance levels, which can be introduced at the appropriate below-threshold points.

The results of the R ratio calculated for the continuum states by including the correction factor $K^{(f)}$ using $\Lambda = \Lambda^{(3)} = 338$ MeV in Eq. (5) for c and b production are shown as the solid curve in Fig. 3 and are compared with the experimental data [26]. The R ratio

obtained just from the tree-level diagram without the correction factor is also shown as the dashed curve. The results of Fig. 3 show that the inclusion of the correction factor gives a good description of the general features of the R ratio. The experimental R ratio and the corrected ratio R are much greater than the tree-level results, near the threshold region. The large enhancement of heavy-quark production is consistent with experimental data, lending support to the predictions of Fig. 1 and Fig. 2 for $t\bar{t}$ production.

The exhaustive fits to the energy dependence of R beyond charm threshold by Barnett et al [17] also used the interpolation formula due to Schwinger and included the low energy dependence of the cross section through an inverse velocity term. They used smearing procedures for proper match between theory and experimental data above the threshold and investigated new hypothetical particles. They expect their threshold results to be unreliable due to their inclusion of the distortion effect only up to the first order in α_s . In the present work, we incorporate the distortion corrections to all orders of the coupling constant on the one hand and we interpolate to the massless quark limit on the other hand. The simple analytical semi-empirical correction factor $K^{(f)}$ of Eq. (10) obtained with only a Coulomb-like potential reproduces the gross features of R over a coarse mesh of energy, as the energy scale of Fig. 3 and the need for the smearing procedure of Ref. [17] will indicate. In finer energy resolutions, the experimental R ratio is modulated by the presence of resonances above the continuum threshold which necessitates the description with a more refined potential including the additional influence of the long-range part of $Q\text{-}\bar{Q}$ interaction, as discussed well in Refs. [22,33,34]. The agreement of our results with the gross features of the experimental R ratio adds credence to the approximate validity of the calculated $t\bar{t}$ production results.

VI. DISCUSSION.

The importance of utilizing the largest possible cross section for top production is self evident. In the light of possible manifestations of new physics expected for the top era [3–5]

and Standard Model violating effects [6], it is important to have a meaningful sample of top events. It is also imperative to have a clear quantifications of Standard Model predictions to enable clean extraction of exotic physics signals. Our distortion corrected cross sections provide the expected top yield within the framework of the Standard Model and can serve as the correct reference to probe new physics frontiers that might be discernible beyond the top threshold.

The large top mass introduces another feature of interest that merits discussion. This is the coupling of the Higgs boson to the $t\bar{t}$ pair, that is manifested as exchange of the scalar Higgs boson between the members of the produced pair. Such an exchange leads to an additional attractive potential between the t and \bar{t} that takes the Yukawa form and can be written [35]

$$V_H(r) = \frac{1}{4\pi} \left(\frac{m_t}{v} \right)^2 \frac{e^{-m_H r}}{r},$$

where m_H and v are the mass and the vacuum expectation value of the Higgs. This is expected to enhance the attractive effects of gluon exchange in the color singlet combination. However in the absence of reliable predictions for the Higgs mass, inclusion of these effects may be premature. Projections for Higgs effects have been carried out by [9].

The possibility of toponium states bound in the pure Higgs potential could also arise. Bounds for the exchanged particle mass, to allow for bound states in a Yukawa potential can be estimated [36,35]. The present lower limit of 60 GeV for the Higgs mass [20] rule out any exclusive bound states in the Higgs potential for t and \bar{t} of the detected mass range.

Finally a comment on possible variations in the top width seems called for. It is well known that initial state binding and masses of the decay products are connected to the effective decay rate of a fermion [37,38]. Since in this case, the binding energy of the decaying top to its production partner, \bar{t} , is of the order of 0.1 GeV only, these effects are small and expected to be beyond the sensitivity range of experimental access at this time. The influence of momentum dependence on the top width and production has been addressed recently [39].

It may be pointed out that the enhancement due to the exclusive color-singlet $t\bar{t}$ formation in electroweak production will not occur in $q\bar{q}$ annihilation processes in $p\bar{p}$ and pp collisions at Tevatron and LHC. Nevertheless, the influence of distortion effects in these environments merits a discussion. The gluon mediated $q\bar{q} \rightarrow Q\bar{Q}$ process is suppressed by the distortion correction [25] due to the repulsive color-octet nature of the one-gluon exchange potential between q and \bar{q} at the initial vertex and between Q and \bar{Q} in the final vertex. However the magnitude of this suppression is much smaller than the enhancement for the color-singlet electroweak channels because of the different color factors for the two cases. The distortion effects are not as striking for QCD vector boson mediated $q\bar{q}$ processes as for electroweak boson mediated ones. However in hadronic and nuclear collisions, $q\bar{q}$ processes are in any case suppressed compared to gluon induced ones. We are investigating the distortion corrections on the gluon fusion channels in a separate work.

We reiterate the justification of the use of the perturbative color potential as acting between both bound and continuum states due to the double influence of the large virtuality of the process, corresponding to contributing distances of order $1/m_t$ and the large top decay rate which serves to kill the top before it can dress itself or cover the wider range of toponia levels. Our results, using the experimentally reported top mass can be used directly for projections of top flavored event rates at the proposed New Linear Collider (NLC) facility and may help to select the most efficient colliding energies for productive top hunting by e^+e^- annihilation.

ACKNOWLEDGMENTS

This research was supported by the Division of Nuclear Physics, U.S. Department of Energy under Contract No. DE-AC05-84OR21400 managed by Martin Marietta Energy Systems, Inc. One of us (LC) would like to thank F. Plasil and M. Strayer of Oak Ridge National Laboratory for their kind hospitality, and University Grants Commission of India for partial support. The authors would like to thank T. Barnes, W. Bugg, E. Hart, Y.

Kamyshkov, K. Read, and S. Willenbrock for helpful discussions.

REFERENCES

- [1] F. Abe et al.(CDF Collaboration). Phys. Rev. Lett. **73**, 220 (1994)
- [2] See e.g. P. Chen, T. L. Barkow, and M. E. Peshkin, Phys. Rev. **D49**, 3209 (1994).
- [3] E. Eichten and K. Lane, Phys. Lett. **B327**, 129 (1994).
- [4] G. A. Lansky and C.-P. Yuan, Phys. Rev. **D49**, 4415 (1994).
- [5] C. T. Hill and S. J. Parke, Phys. Rev. **D49**, 4454 (1994).
- [6] W. Bernreuther and A. Brandenburg, Phys. Rev. **D49**, 4481 (1994).
- [7] E. Laenen, J. Smith and W.L. Van Neerven, Phys. Lett. **B321**, 254 (1994).
- [8] V. Fadin, V. Khose and T. Sjöstrand, Zeit. Phys. **C48**, 613 (1990).
- [9] M.Strassler and M.E. Peskin, Phys. Rev. **D43**, 1500 (1991).
- [10] W. Kwong, Phys. Rev. **D43**, 1488 (1991).
- [11] Y. Sumino, K. Fujii, K. Hagiwara, H. Murayama, C.K. Ng, Phys. Rev. **D47**, 56 (1993)
- [12] F.J. Yndurain, Phys. Lett **B 321**, 400 (1994).
- [13] W. Beenakker, H. Kuijf and W.L. Van Neerven, Phys. Rev. **D40**, 54 (1989). W. Beenakker, W. L. van Neerven, R. Meng, G. A. Schuler, and J. Smith, Nucl. Phys. **B351**, 507 (1991).
- [14] P. Nason, S. Dawson, and R. K. Ellis, Nucl. Phys. **B303**, 607 (1989).
- [15] P. Nason, S. Dawson, and R. K. Ellis, Nucl. Phys. **B327**, 49 (1989).
- [16] T. Applequist and H. D Polizer, Phys. Rev. Lett. **34**, 43 (1975); Phys. Rev. **D12**, 1404 (1975).
- [17] R. M. Barnett, M. Dine and L. McLerran, Phys. Rev. **D22**, 594 (1980).
- [18] S. Güsken, J. H. Kühn and P.M. Zerwas, Phys. Lett. **155B**, 185 (1988).

- [19] V. Fadin and V. Khose, Soviet Jour. Nucl. Phys. **48**, 487 (1988).
- [20] L. Montanet *et al.*, Particle Data Group, *Review of Particle Properties*, Phys. Rev. **D50**, 1173 (1994).
- [21] R. D. Field, *Applications of Perturbative QCD*, Addison-Wesley Publishing Company, 1989.
- [22] E. Eichten, K. Gottfried, T. Kinoshita, K.D. Lane and T. M. Yan, Phys. Rev. **D17**, 3090 (1978); **D21**, 313(E) (1980); **D21**, 203 (1980).
- [23] E. Eichten and C. Quigg, Phys. Rev. **D49**, 5845 (1994).
- [24] A. I. Akhiezer and V. B. Berestetskii, *Quantum Electrodynamics*, Interscience Publishers, New York, 1965.
- [25] L. Chatterjee and C. Y. Wong, hep-ph@xxx.lanl.gov Preprint 9412349, (Oak Ridge National Report ORNL-TH-941201).
- [26] K. Hikasa *et al.*, Particle Data Group, *Review of Particle Properties*, Phys. Rev. **D45**, S1 (1992).
- [27] G. Gamow, Zeit. Phys. **51**, 204 (1928); A. Sommerfeld, *Atmobau und Spektralinien*, Bd. 2. Braunschweig: Vieweg 1939.
- [28] J. Schwinger, *Particles, Sources, and Fields*, (Addison-Wesley, New York, 1973), Vol. II, Chap. 4 and 5.
- [29] I. Bigi, Y. Dokshitzer, V. Khose, J. Kuhn and P. Zerwas, Phys. Lett. **B181**, 157 (1986).
- [30] S. Abachi *et al.* (D0 Collaboration). Phys.Rev. Lett. **72**, 2138 (1994).
- [31] B. Pietrzyk for LEP Collaborations and the LEP Electroweak working group, Laboratoire de Physique des Particules, Report No LAPP-EXP-94.07 (1994).
- [32] C. G. Arryo *et al.* Phys. Rev. Lett. **72**, 3452 (1994).

- [33] V. Zambetakis, UCLA Ph. D. Thesis (1985), UCLA Report UCLA/85/TEP/2.
- [34] N. Buers, hep-ph@xxx.lanl.gov Preprint 9412292, (UCLA Report UCLA/94/TEP/47),
to be published in the Proceedings of International Conference on Quark Confinement
and Hadron Spectrum, Villa Olmo-Como, Italy, June 1994.
- [35] H. Inazawa and T. Morii, Phys. Lett. **B203**, 279 (1988).
- [36] C. Y. Wong, *Introduction to High-Energy Heavy-Ion Collisions*, World Scientific Pub-
lishing Company, 1994.
- [37] L. Chatterjee, A. Chakrabarty, G. Das, and S. Mondal, Phys. Rev. **D46**, 5200 (1992).
- [38] L. Chatterjee and V. P. Gautam, Phys. Rev. **D41**, 1698 (1990).
- [39] M. Jezabek, J. H. Kuhn, T. Tuebner, Zeit. für Phys. **C56**, 653 (1992).

FIGURES

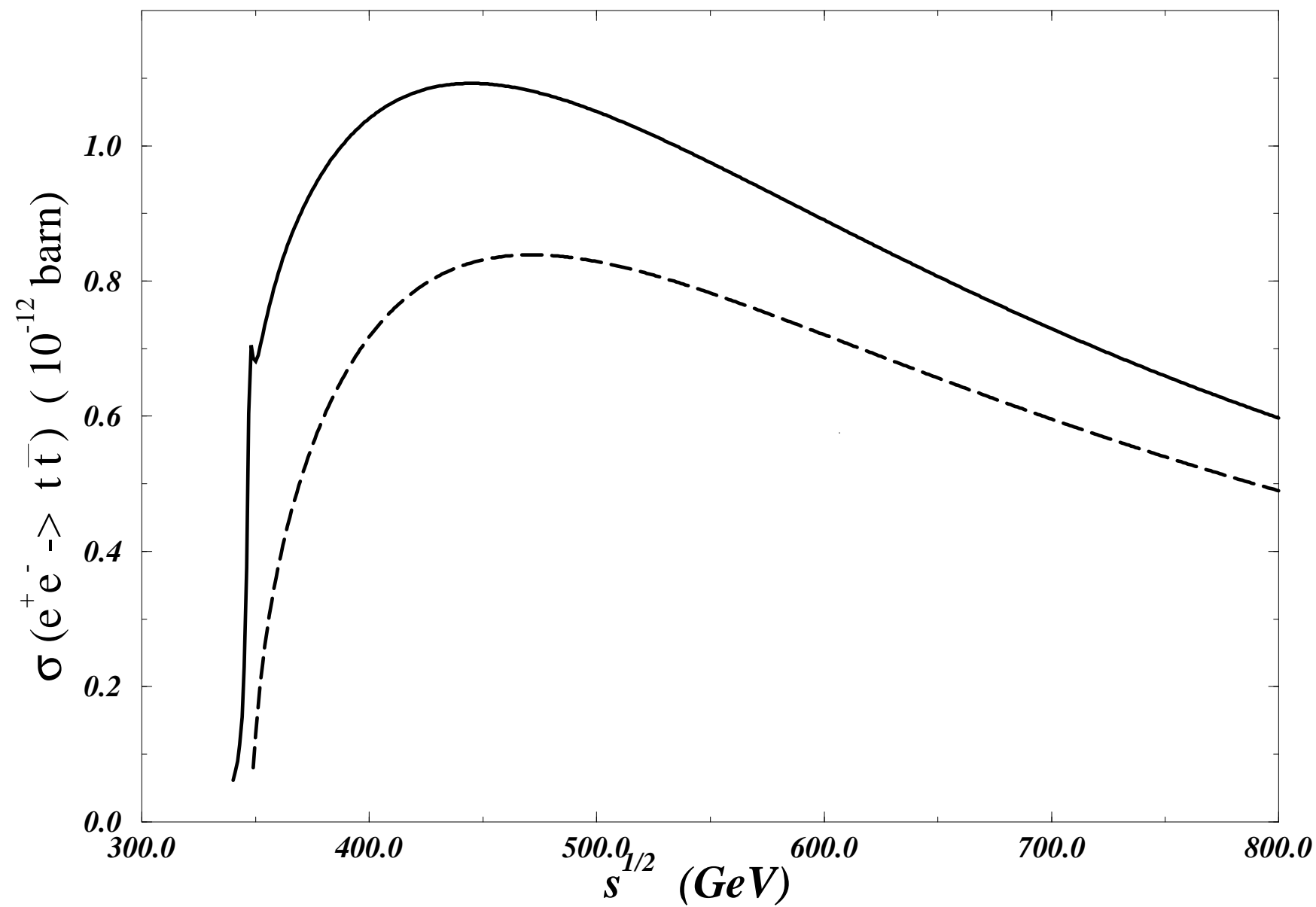
FIG. 1. The cross section for $e^+e^- \rightarrow t\bar{t}$. The solid curve is the total cross section by including the bound and continuum states, and the correction factor $K^{(f)}$. The dashed curve is obtained from the tree-level diagram for the continuum states.

FIG. 2. The cross section for $e^+e^- \rightarrow t\bar{t}$ near the threshold region. The solid curve is the total cross section by including the bound states and the continuum states. The dot-dashed curve and the long-dashed curve are obtained from the bound states and the continuum states respectively.

FIG. 3. The ratio R as a function of the center-of-mass energy \sqrt{s} . The solid curve is the result obtained by including the correction factor $K^{(f)}$, and the dashed curve is from the tree-level diagram. The data points are from the compilation of Ref. [26].

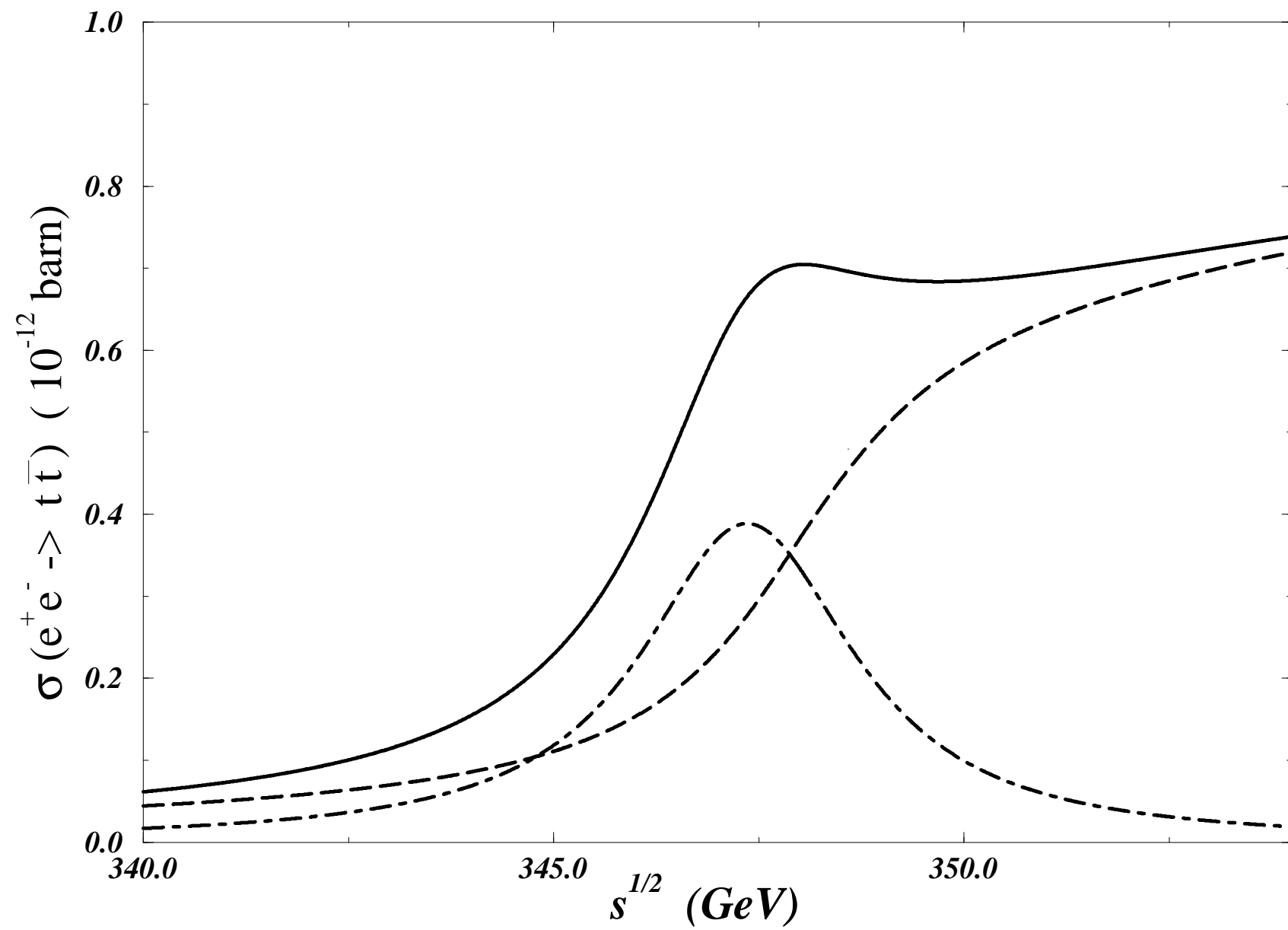
This figure "fig1-1.png" is available in "png" format from:

<http://arxiv.org/ps/hep-ph/9501218v1>



This figure "fig1-2.png" is available in "png" format from:

<http://arxiv.org/ps/hep-ph/9501218v1>



This figure "fig1-3.png" is available in "png" format from:

<http://arxiv.org/ps/hep-ph/9501218v1>

